Theses and Dissertations

12-2017

Structural and Elastic Properties of Degenerate SnO Monolayers at Finite Temperature

Afsana Sharmin
University of Arkansas, Fayetteville

Structural and Elastic Properties of Degenerate SnO Monolayers at Finite Temperature

A thesis submitted in partial fulfillment
of the requirements for the degree of
Master of Science in Physics

by

Afsana Sharmin
University of Dhaka
Bachelor of Science in Applied Physics, Electronics &
Communication Engineering, 2007
Southern Illinois University Carbondale
Master of Science in Electrical and Computer Engineering, 2013

December 2017
University of Arkansas

This thesis is approved for recommendation to the Graduate Council

_____
Dr. Salvador Barraza-Lopez
Thesis Director

_____   _____
Dr. Surendra P. Singh   Dr. Hugh Churchill
Committee member   Committee member

ABSTRACT

Chalcogen-based layered superconductors with a litharge structure such as FeS and FeSe mono-layers undergo structural and superconducting phase transitions that are tunable by doping. Representing another material platform with a litharge structure but without valence d-electrons, SnO monolayers also display a structural ground state with a degenerate rectangular unit cell at zero temperature and a charge-tunable energy barrier that leads to a thermally-controllable structural phase change. Doped SnO monolayers with rectangular degenerate unit cells give rise to two-dimensional multiferroicity. Their two-dimensional elastic energy landscape adopts a basic analytic expression that is employed to discuss this structural transition. The results contained in this thesis increase our intuition on two-dimensional phase transitions and their effects on the properties of two-dimensional atomic materials with structural degeneracies.

TABLE OF CONTENTS

CHAPTER 1

INTRODUCTION

Imagine one can read the newspaper on a cup at breakfast time, watch a TV screen hanging on the wall which has a thickness less than that of a sheet of paper, use a cell phone less than a millimeter thick while being much faster and less power consuming than the current cell phones. These are some of the potential applications of some recently discovered two dimensional materials which are one atom thick. These new materials may transform these ideas into reality one day. Among 2D materials, SnO has potential in catalysis, coatings and as a lithium-ion storage material too [1]. Other than these electronic applications, SnO becomes a superconductor under pressure.

Degenerate structural ground states are a staple of soft-condensed matter systems. Structural degeneracies lead to phase transitions at a temperature that is proportional to the smallest energy barrier separating these degenerate structures [2]. In a similar manner, a six-fold degenerate ground state is the workhorse of many bulk ferroelectric [3] and multiferroic [4] materials.

Here, we study SnO monolayers to continue our understanding towards a complete picture of how properties of two-dimensional materials are affected by two dimensional structural transitions at finite temperature. SnO monolayers share the paradigmatic litharge structure of iron-based superconductors FeS and FeSe. But lacking d-electrons and superconductivity under atmospheric pressure conditions, SnO appears as a more straightforward vehicle to initiate a discussion related to structural transitions.

The existence of a ground state structure with a rectangular unit cell on α-SnO [5] provides a new platform for an emerging discussion of two-dimensional structural phase transitions on materials with rectangular unit cells [6-8]. SnO also has a charge tunable energy barrier which can lead to a controllable structural phase change and this phenomenon can be studied analytically. The analytical model yields the transition temperature, $Tc,$ captures the sudden change in the structural order parameters, the elastic energy, and elastic parameters.

CHAPTER 2

2D MATERIALS

2.1 2D Materials History and Impact

There were different theories and efforts to investigate the possibility of the existence of two dimensional materials for a long time. However, in 2004, Graphene was the first 2D material to be exfoliated. [9] Based on the bulk material that has been used to create 2D materials, they can be classified into two main classes: 1) Van der Waals 2D materials and, 2) layered ionic solids. Van der Waals 2D materials are the most common form [10]. These materials are created by mechanical or chemical exfoliation of their bulk material.

In their bulk form, these materials are stacked layers arranged with van der Waals forces (hence their name) [11]. Examples of this kind of 2D materials are graphene, hexagonal boron nitride [12], and phosphorene [13]. Graphene and phosphorene have strong covalent bonds between atoms in one layer. The atomic bonds in each layer can also be ionic. Due to weak van der Waals interaction between layers, these solids can be easily exfoliated. Metals (M) such as titanium, zirconium, hafnium, vanadium, niobium, and tantalum with chalcogens (elements in group six of the periodic table) — mostly sulfur, tellurium, and selenium (usually labeled X) — are the most common and studied form of other van der Waals 2D materials with chemical formula MX_2. MoS_2 [14], $TiSe_2$ and WSe_2.

The second class of 2D materials is called layered ionic solids [15]. The atoms in a single layer of these materials are bound together with strong electrostatic bonds. Most of these 2D materials are metallic oxides, for instance TiO_2, SnO, MnO_2 and $Ni(OH)_2$.

2.2 Properties of 2D Materials

In 2D materials, electrons are confined in a surface rather than a 3-dimensional space. The interaction between layers of bulk materials plays a significant role in their electronic and optical properties [16]. By confining interactions to two dimensions, new electronic behavior is observed (such as Hall effects) which has made researchers optimistic to exploit these properties and make new electronic devices. Another difference of 2D materials compared to bulk 3D materials is the effect of shape and stacking on their properties. For example, the properties of a single layer of graphene are different from those of 2 layers and they are still different from 3 layers of graphene [17]. Even relative stacking angular mismatches play a role in electronic properties [13]. Elastic deformation also changes material properties. For instance, strain changes the properties by altering the orbital hybridization [18]. Some 2-dimensional materials are good thermal conductors. For example, 2D Boron Nitride is reported to have a thermal conductivity in the range of 100-270 $\mathrm{W/mK}$ [19] due to an absent phonon scattering from subsequent layers [20].

2.3 Lattice Structure of SnO

The crystal structure of a SnO monolayer has orthorhombic symmetry. The Oxygen atoms are arranged in a planar square sub-lattice and the tin atoms are arranged in alternating pyramids with square bases bounded by the oxygen atoms. By using first principles calculations, the lattice constant for charge neutral SnO monolayer with ground state structure has been found $a_{1L} =$ 4.021667245 A^0 and $a_{2L} = 3.656934052 \ \mathrm{A}^0$. So this ground state structure is rectangular, rather than litharge structure.
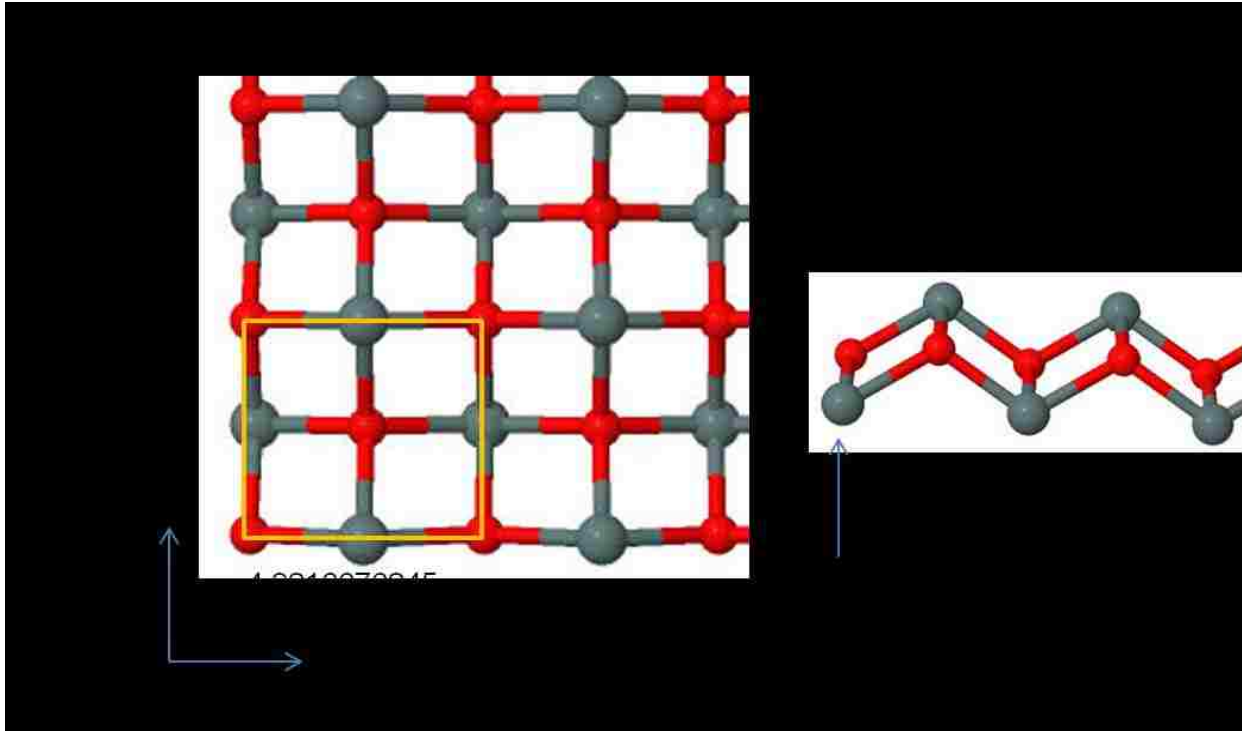
Figure 2.1 SnO monolayer from (A) top view (Top panel) and (B) side view (Bottom Pannel)

2.4 Scope of the Work

The objective of the thesis is to provide numerical data that will eventually lead to an analytical model for the two-dimensional elastic energy landscape of SnO. The specific contributions of this thesis are: (1) to discuss the properties of pre and post structural transition of neutral SnO monolayer such as the transition temperature Tc, which is signaled by a sudden change in the structural order parameters, the elastic energy, and elastic parameters, and (2) how doping of SnO monolayer has effect on its energy landscape. The thesis is organized into the following chapters.

Chapter 1 provides the motivation for this research.

Chapter 2 provides a brief introduction to the history and properties of 2-D materials and lattice structure of SnO monolayer.

Chapter 3 provides the first principle calculations using VASP where the input files such as INCAR, KPOINTS, POSCAR, and POTCAR have been described. It also describes the elastic energy of SnO monolayer as a function of strain.

Chapter 4 focuses on results. It explains the elastic energy of SnO monolayer for charge neutral slab and also gives information for transition temperature. It also provides explanation of the elastic energy of SnO monolayer with hole and electron doping.

Chapter 5 summarizes the presented work in this thesis and provides suggestions for future work.

CHAPTER 3

FIRST PRINCIPLES CALCULATIONS USING VASP FOR SnO MONOLAYERS

In this thesis, first principles calculations have been done based on density functional theory (DFT) by using the Vienna Ab Initio Simulation Package (VASP). Electronic wavefunctions are expanded on a plane wave basis set. First, the first principle calculations for the neutral slab of SnO monolayer without strain have been done and the elastic energy is calculated without strain and without doping. Then the elastic energy for neutral slab has been calculated as a function of strain. After that, the elastic energy for hole doped and electron doped SnO monolayer has been calculated without strain. Finally, the elastic energy calculations for doped SnO monolayer have been done as a function of strain. Elastic energy of the material can be described as the potential mechanical energy stored in the configuration of a material as work is performed to distort its volume or shape. Elastic energy is stored on the material when objects are compressed and stretched, or generally if there is a deformation in any manner.

3.1 Input Files

Most calculations have been done for SnO monolayer in a work directory. Before starting the calculations, several files have been created in this directory. The important input files are

INCAR   KPOINTS, POSCAR and POTCAR

These four files are the central input files, and must exist in the work directory before VASP can be executed.

3.1.1 K-Points

The file KPOINTS contains k-point coordinates or mesh size for creating the k-point grid [21]. The k-points samples in the Brillouin zone are calculated with the $\Gamma-$centered with 15x15x1

for SnO monolayers. In our thesis, automatic generation has been used to generate k-meshes. For SnO monolayer, K-points file looks like the following way:

Automatic mesh

0   ! number of k-points = 0 ->automatic generation scheme

Gamma   ! generate a Gamma centered grid

15 15 1   ! subdivisions N_1, N_2 and N_3 along recipr. l. vectors

0. 0. 0.   ! optional shift of the mesh (s_1, s_2, s_3) .

3.1.2 INCAR

The INCAR file is the central input file of VASP. It determines 'what to do and how to do it'. It is a tagged format file: Each line consists of a tag with the equation sign '=' and one or several values [21]. The INCAR file has been modified in our thesis to create the SnO monolayer - neutral or doped with electrons or holes. SnO unit cells have a total number of 4 atoms and 20 electrons. For the neutral SnO monolayer, the NELECT has been kept as 20.00, for electron doping it goes from 20.01 to 20.1 this and for hole doping the calculation has been done from 19.95 to 19.55. Ionic steps of 400 have been kept as NSW=400. The energy cutoff is supplied in the INCAR file and in all cases, ENCUT = 500 has been kept. For all the cases, EDIFFG = -1E-3 has been kept which is the stopping criteria for ionic accuracy. In the same way for all the cases, EDIFF = 1E-7 has been kept which is the accuracy for electronic minimization. In the INCAR file, ISIF controls how the stress tensor is calculated. ISIF determines which degrees of freedom (ions, cell volume, and cell shape) are allowed to change. When the calculations for strain have been done, ISIF =2 was given. It means that the ions can relax but cell shape cannot change. When the calculations have been done for without strain, ISIF=4 was given and it means that ions can relax and cell shape can change. ISMEAR = 0 has been chosen here so that Gaussian smearing can be chosen for the partial occupancies for each wave function [21].

3.1.3 POSCAR and POTCAR

The POSCAR file contains the lattice geometry and the ionic positions. In POSCAR, the following information has been provided to obtain the ground state of neutral SnO monolayer:

Lattice geometry:

1.00000000000000

4.0216676245000000   0.0000000000000000   0.0000000000000000

0.0000000000000000   3.6569340451999999   0.0000000000000000

0.0000000000000000   0.0000000000000000   9.8111553800221625

Sn   O

2   2

Selective dynamics

Ionic Position of Sn and O:

0.0000000000000000 0.5000000000000000 0.3904290833675363

0.5000000000000000 0.0000000000000000 0.6296078454341303

0.0000000000000000 0.0000000000000000 0.5200376022584215

0.5000000000000000 0.5000000000000000 0.5000000000000000

The POSCAR file also contains the number of atoms per species which is for this SnO POSCAR file two tin atoms and two oxygen atoms. So, from the POSCAR file, it can be seen that the ground state is rectangular structure. This SnO rectangular structure undergoes a structural transition in which the two dissimilar in-plane lattice parameters acquire an identical magnitude at a certain transition temperature. So, then it becomes litharge structure.

For the SnO monolayer neutral unit cell with litharge structure, in POSCAR the following information has been provided:

Lattice geometry:

1.00000000000000

3.83561900000000   0.00000000000000   0.00000000000000

0.00000000000000   3.83561900000000   0.00000000000000

0.00000000000000   0.00000000000000   9.83000000000000

Sn   O

2   2

Selective dynamics

Ionic positions of Sn and O:

0.0000000000000000 0.5000000000000000 0.3800469469752632

0.5000000000000000 0.0000000000000000 0.6199530530247368

0.0000000000000000 0.0000000000000000 0.5000000000000000

0.5000000000000000 0.5000000000000000 0.5000000000000000

At the end of each job, VASP writes the final positions to the CONTCAR file. This file has the same format as the POSCAR file, and the calculations can be done by copying CONTCAR to POSCAR and running VASP again for continuation of the jobs.

The POTCAR file contains the pseudopotential for each atomic species of SnO used in the calculation. The POTCAR file also contains information about the SnO atoms such as their mass, their valence, and the energy of the reference configuration for which the pseudopotential was created [21].

3.2 Elastic Energy of SnO-Monolayer as a Function of Strain

First, the elastic energy of charge neutral SnO monolayer without strain has been assessed and for this case ions can relax as well as cell shape can change. After that, the elastic energy of charge neutral SnO monolayer has been assessed varying the lattice constants where the unitary strain has been applied ranging from $\pm0\%$ up to $\pm10\%$ with an interval of 0.25%. The ground state of the charge neutral SnO monolayer has been recorded. The litharge structure state energy has also been recorded for the neutral SnO. For p-type SnO material, the elastic energy without strain has been assessed for hole doping at 0.05, 0.25, 0.35 and 0.45. After that, similar

unitary strain like the charge neutral slab has been applied for hole doped SnO from ±0% up to ±10% at an interval of 0.25%. Then for those p-type materials, the ground state energy and litharge state energy have been recorded. For n-type SnO material, without strain elastic energy has been assessed for electron doping of 0.01, 0.02, 0.03, and 0.04. Finally same unitary strain like charge neutral slab has been applied for electron doped SnO and ground state energy and litharge state energy have been recorded. In the following chapter, all the results for charge neutral, hole doped and electron doped SnO monolayer have been described.

CHAPTER 4

RESULTS AND DISCUSSION

4.1 Elastic Energy of Charge Neutral SnO-Monolayer

The elastic energy landscape for the SnO monolayer with zero doping has been shown in the following Figure 4.1 (b). From the simulation, it has been realized that a SnO monolayer does not possess a litharge structure (with identical in-plane lattice vectors a_1 and a_2) at zero temperature. Instead its ground state structure is rectangular.

Two dimensional materials with rectangular unit cells $(a_1 > a_2)$ lead to a clear structural degeneracy as the elastic energy $U(a_1, a_2)$ remains invariant under exchange of lattice vectors: $U(a_1, a_2) = U(a_2, a_1)$. So the Structural degeneracy of this structure is two-fold. This fact is illustrated in Figure 4.1 (a) for an undoped SnO monolayer following the notation introduced in [5]. In Figure 4.1 (a), the ground state at the energy minima $(a_1 > a_2)$ is labeled A (with elastic energy $U_A = U(a_1, a_2)$) and the ground state at the energy minima ($a_2 > a_1$) is labeled B (with elastic energy $U_B = U (a_2, a_1)$) and $U_A = U_B$. The litharge structure $(a_1 = a_2 = a_0)$ is labeled C (with elastic energy $U_C = U(a_0, a_0)$) and $U_C > U_B$.

As seen in Figure 4.1(b), the minimum energy required to turn SnO from structure A onto structure B is given by $= U(a_0, a_0) - U_A = U_C - U_A$ where C is the middle point between A and B.
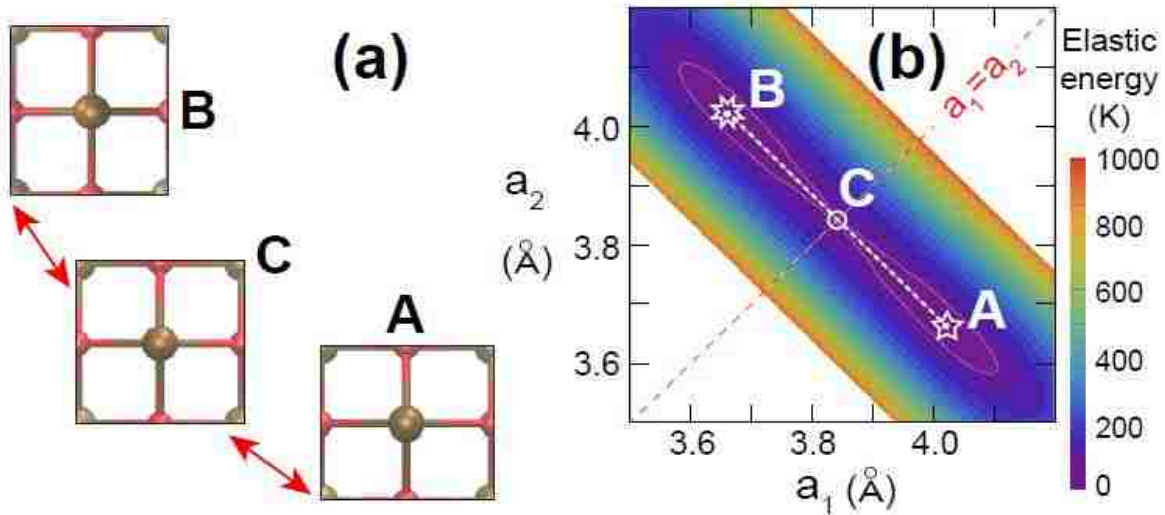
Figure. 4.1. (a) Unit cell structure of SnO at the energy minimum (structure A) and with a litharge structure (structure C), (b) Elastic energy landscape for the SnO monolayer with zero doping

So, in Figure 4.1(a), the unit cell of SnO has shown with a litharge structure titled as structure C and structure A and B are showing the energy minimum rectangular structures. In the absence of doping, these materials do not possess an intrinsic magnetic moment (M = 0). Then, density-functional theory calculations yield the elastic energy shown in Figure. 4.1.

The orthogonal variables x and y are functions of lattice parameters a_1 and a_2 as follows:

$x = \frac{a_1 - a_2}{\sqrt{2}}$ and $y = \frac{a_1 + a_2 - 2a_0}{\sqrt{2}}$ (4.1)

These orthogonal variables capture the symmetry of the energy profile in Figure 4.1(b), as shown by the dashed white (x) and red (y) lines at -45^0 and $+45^0$ with respect to a_1 axis.

This elastic energy fitting can be described analytically as:

$U(x, y) = ax^4 - bx^2 + cy^2 + \frac{b^2}{4a}$ (4.2)

Where a, b and c are real and positive parameters. The values are a = 0.3664 eV/A⁴, b = 0.0475 eV/A² and c = 1.9564 eV/A² for a slab with no doping. A cut of the energy profile along the y = 0 line is shown in Figure 4.2.
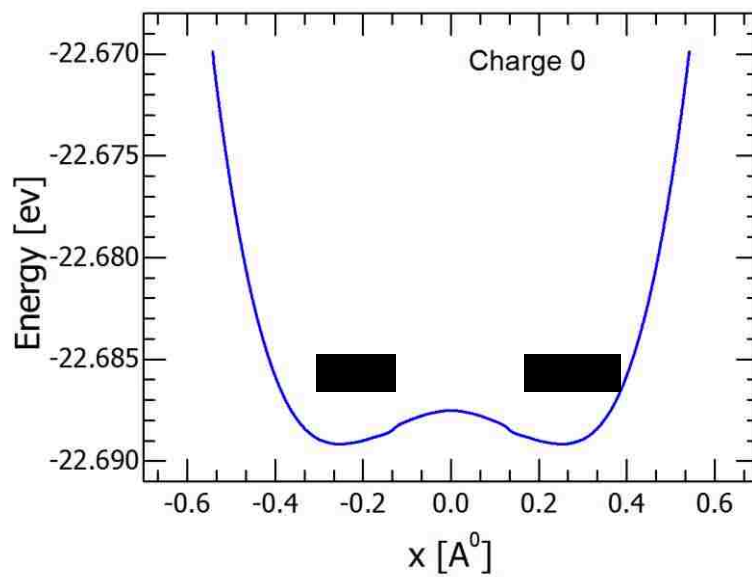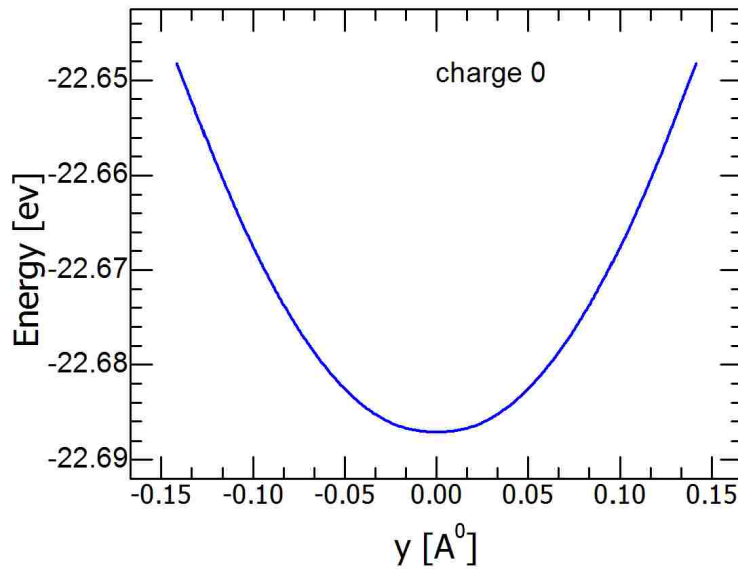
Figure. 4.2. Elastic energy without doping for y=0

. A cut of the energy profile along the x = 0 line and x with a constant line at minima are shown in figure 4.3 and 4.4.
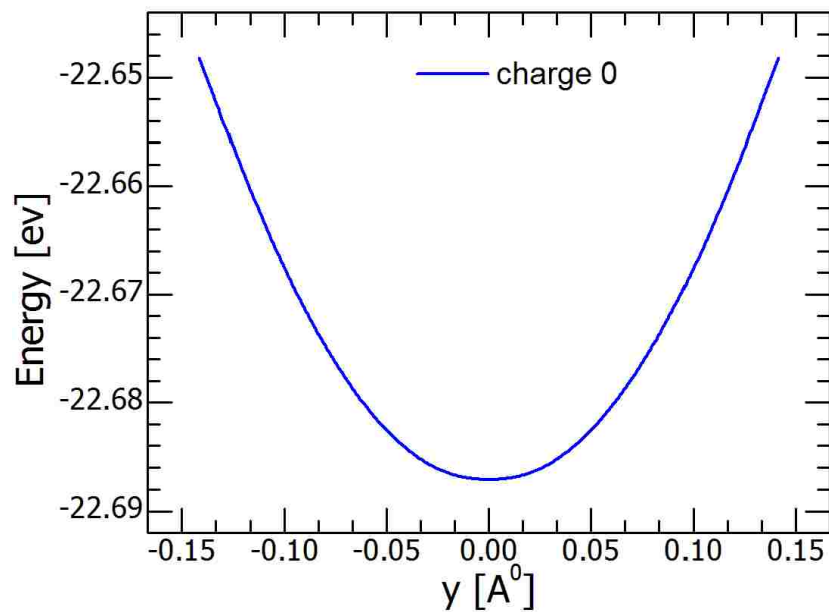
Figure 4.3. Elastic energy without doping for x=0

Figure 4.4. Elastic energy without doping for a constant x at minima

Previous order four and hence anharmonic expression for the energy [22] yields two minima at points (a_{10}, a_{20}) and (a_{20}, a_{10}) and a point of unstable equilibrium C at $(x_c, y_c) = (0,0)$ or $(a_1, a_2) = (a_0, a_0)$ with $a_0 = 3.8393$ A^0 , $a_{10} = 4.0217$ A^0 and $a_{20} = 3.6569$ A^0 for a charge neutral slab.

$U(x, y)$ is normalized such that $U(x_0, y_0) = 0$, and it provides an energy scale given by the energy difference between the saddle point C and the energy minima:

$$\Delta U = U(0,0) - U(x_0, y_0) = \frac{b^2}{4a} \tag{4.3}$$

The elastic energy profile given by equation (4.2) has two dimensional dependence on strain, as the shape of Figure 4.1(b) depends on both the anti-diagonal and diagonal strain (i.e., the variable y complements the model provided in Ref. [5] in which the strain component employed is the anti-diagonal one; $\epsilon = \epsilon(x)$).

Now, the elastic energy in terms of the unitary strains $\epsilon_{11} = \epsilon_{22}$ can be expressed. Two considerations must be sorted out for this expression.

(1) Without known exceptions, unitary displacements in elasticity theory are always referred with respect to a local minima (a position of stable equilibrium), not with

respect to points of unstable equilibrium as the saddle point C from figure 4.1(b) employed in [5] to define $\epsilon_{xx} = \epsilon_{yy} = 0$.

(2) Given that the SnO structure is two-fold degenerate, any of the minima should be employed to express $\epsilon_{xx} = \epsilon_{yy} = 0$.

Figure 4.1 illustrates conditions (1) and (2) at play on the SnO monolayer, and a local minima has been chosen at $(x_0, y_0) = (+\sqrt{\frac{b}{2a}}, 0)$, and hence assumes the existence of a macroscopically large mono-domain with configuration A in Figure 4.1(a). In this case, Equation (4.1) can be expressed x and y in terms of the lattice parameters at the local minima A and unitary strains $\epsilon_{11} = \epsilon_{22}$ as follows:

$$a_{10} = a_0 + \frac{1}{2}\sqrt{\frac{b}{a}} \text{ , and } a_{20} = a_0 - \frac{1}{2}\sqrt{\frac{b}{a}} \tag{4.4}$$

where , $\epsilon_{11} = \frac{a_1 - a_{10}}{a_{10}}$, $\epsilon_{22} = \frac{a_2 - a_{20}}{a_{20}}$, so

$$x = \frac{a_{10}(1+\epsilon_{11}) - a_{20}(1+\epsilon_{22})}{\sqrt{2}}, \text{ and } y = \frac{a_{10}(1+\epsilon_{11}) + a_{20}(1+\epsilon_{22}) - 2a_0}{\sqrt{2}} \tag{4.5}$$

The two-dimensional dependence of the elastic energy upon in-plane strain is realized by replacing x and y in Equation (4.2) by Equation (4.5).

Assuming that the energy profile obtained at zero temperature holds at finite temperature, we bring a classical analogy of a particle on a two-well system to action, and assign a mean kinetic energy equals to $k_B T$, where T is the temperature and k_B is the Boltzmann's constant. Then, since $U(x_0, y_0) = 0$, the structure at the local minima $(x_0, y_0) = (+\sqrt{\frac{b}{2a}}, 0)$ will have a zero elastic energy and a mean $k_B T$ kinetic energy, which will allow it to reach the walls of the confining well up to a height equal to $k_B T$, at which its mean kinetic energy is zero.

$$k_B T = U(x, y) \tag{4.6}$$

For a given T, limits along the x-axis are given by setting $U(x, y) = 0$. Thus equation (4.6) leads to four solutions:

$$x_{N\pm}(T) = -\sqrt{\frac{b\pm\sqrt{4ak_BT}}{2a}}, \; x_{p\pm}(T) = \sqrt{\frac{b\pm\sqrt{4ak_BT}}{2a}} \tag{4.7}$$

where N and P stands for negative and positive. The elastic energy profile, being a classical construct, forbids direct tunneling among the two valleys which have been shown in Figure 4.2 as A and B . Therefore, one is constrained to (x_{min}(T) = x_{P-}(T) $\leq x \leq x_{P+}$(T) = x_{max}(T)) when k_BT$\leq \Delta U$ given the choice of mesoscopic monodomain made. Furthermore, x_{p-}(T) = 0 for $T = \Delta U/k_B$.

Transition temperature, T_c can be extracted from equation (4.6) and it is 19.3K.

As $T > \Delta U/k_B$ both valleys become accessible and the system explores them evenly. For this case, x_{N-} and x_{p-} become imaginary, and the accessible limits in the landscape turn into (x_{min}(T) = x_{N+}(T) $\leq x \leq x_{p+}$(T) = x_{max}(T)). So, $x_{min}(T)$ takes two different values, depending on whether T $\leq \Delta U/k_B$ or T$> \Delta U/k_B$.

4.2 Elastic Energy of SnO with Hole Doping

The structural stability of p-type material has been first assessed. The elastic energy has been calculated by applying strain and varying the lattice constants in x-direction. In this case the ions can relax. Elastic energy has been calculated with hole doping ranging from 0.05, 0.25, 0.35 and 0.45. It has been found from the simulation that elastic energy is a function of charge doping. So, the analytical expression for the elastic energy at zero temperature from equation (4.2) can be rewritten as:

$$U(x, y, q) = |a(q)|x^4 - |b(q)|x^2 + |c(q)|y^2 + d(q) \tag{4.8}$$

Increasing the hole doping ,the energy difference between the ground state energy (rectangular structure) and litharge state energy ΔU can be controlled.
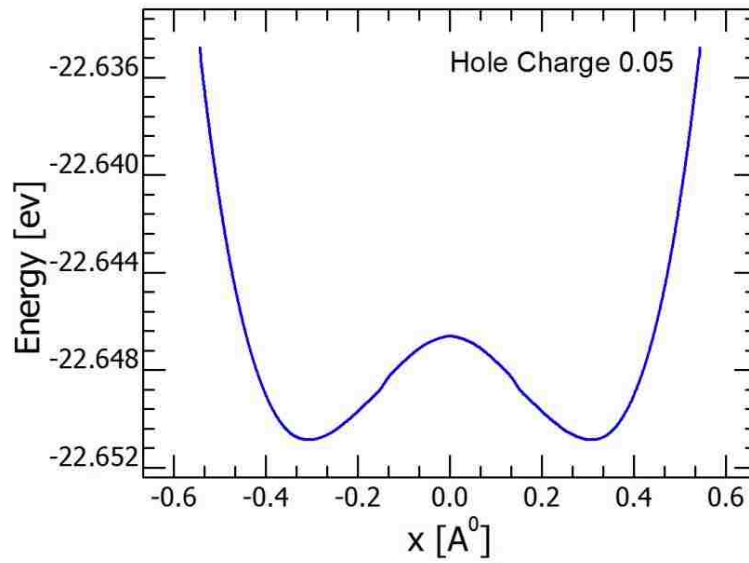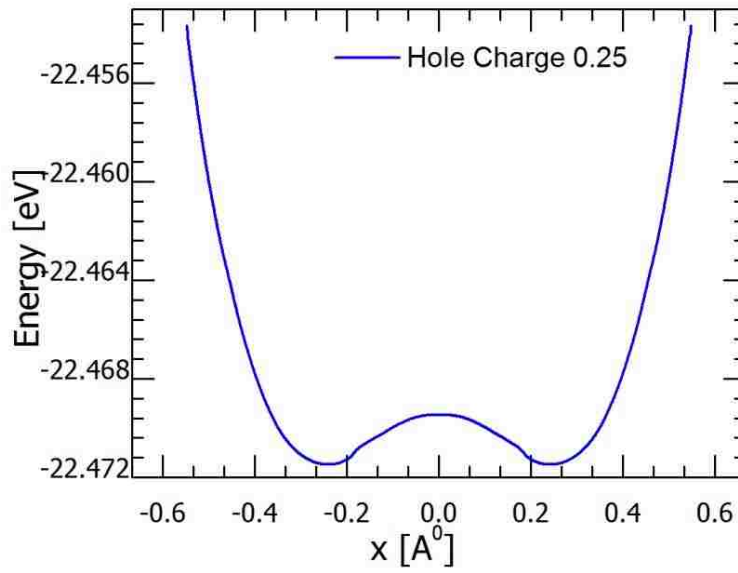
Figure 4.4. Elastic energy with hole doping of 0.05 for y =0

In the Table 1 hole charge per unit cell q, lattice parameters of litharge structure a_0 , litharge structure energy U_0 , optimal rectangular structure (a_1, a_2), ground state energy U_g and energy difference between litharge structure and ground state energy ΔU for SnO monolayer have been provided.

Table 1: q,a_0 with associated energy U_0, (a_1,a_2) with associated energy $U_g$and ΔU (energy difference between U_g and U_0)

$q(e)$	a_0 (A^0)	U_0 (ev)	a_1 (A^0)	a_2 (A^0)	U_g(ev)	ΔU (ev)
0.05	3.846926	-22.64660	4.068124	3.625728	-22.65087	0.00427
0.25	3.878704	-22.46946	4.053246	3.704162	-22.47148	0.00202
0.35	3.893052	-22.37052	3.980646	3.805459	-22.37076	0.00024
0.45	3.906786	-22.26017	3.906786	3.906786	-22.26017	0.000000

Figure 4.5. Elastic energy with hole doping of 0.25 for y =0

By applying strain and varying the lattice constants in x- direction and putting y =0, the coefficients of equation (4.8) a, b and d can be obtained.

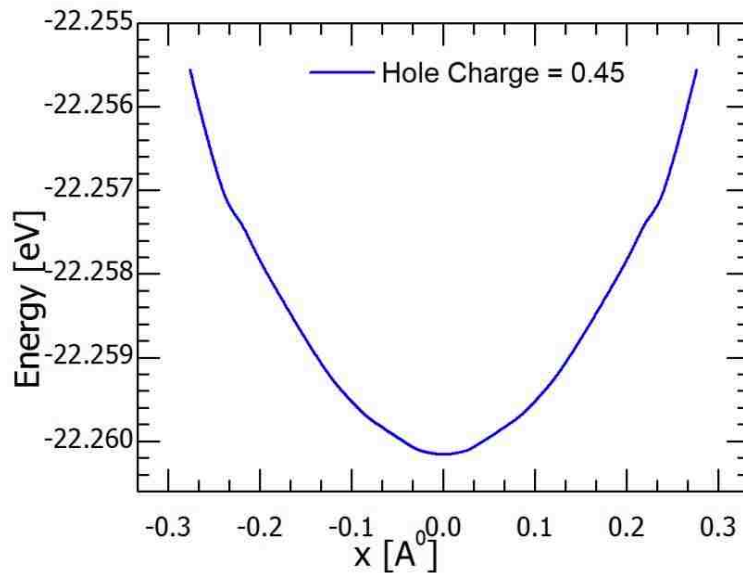The following Table 2 shows the hole charge per unit cell q with associated coefficients.

Table 2: q with associated a, b and d

$q(e)$	$a\ (^{ev}/_{A^4})$	$b(^{ev}/_{A^2})$	$d(ev)$
0.05	0.412800	-0.080100	-22.647000
0.25	0.317500	-0.040400	-22.470000
0.35	0.315900	-0.001400	-22.371000
0.45	0.000000	0.057000	-22.260000
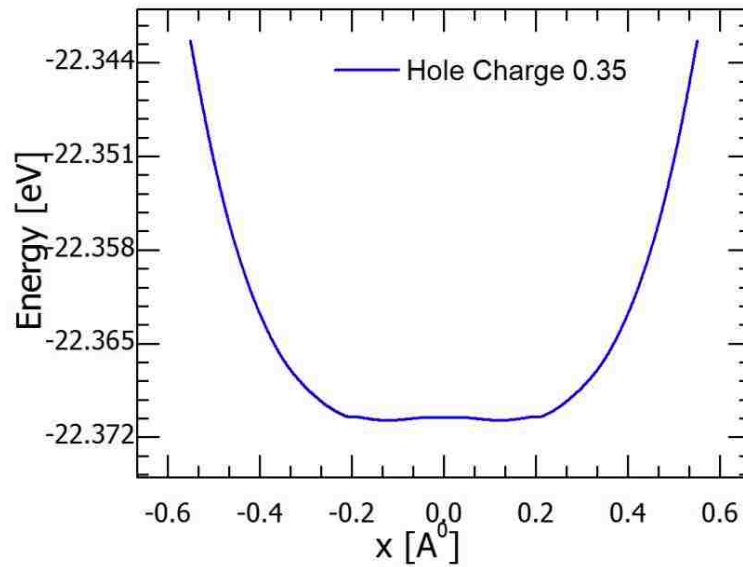
Figure 4.6. Elastic energy with hole doping of 0.35 for y =0

Figure 4.7. Elastic energy with hole doping of 0.45 for y =0

From Table 1, it can be inferred that increasing the hole doping density, ground state energy starts to increase. With the changing hole doping density, the energy difference between ground state and litharge structure state ΔU can be controlled. Since from equation (4.6), it has been shown that the transition temperature T_c is related to ΔU, so T_c can be also controlled with hole doping. As the hole doping has been increased to 0.45, from Table 1 it can be seen that ΔU

becomes zero. That means with hole doping of 0.45, the ground state structure becomes litharge structure. Again from Table 2 it can be seen that with coefficient a=0, that means varying lattice constants in x-direction and putting y =0, the anharmonic analytical expression (4.8) becomes harmonic when hole doping is 0.45.
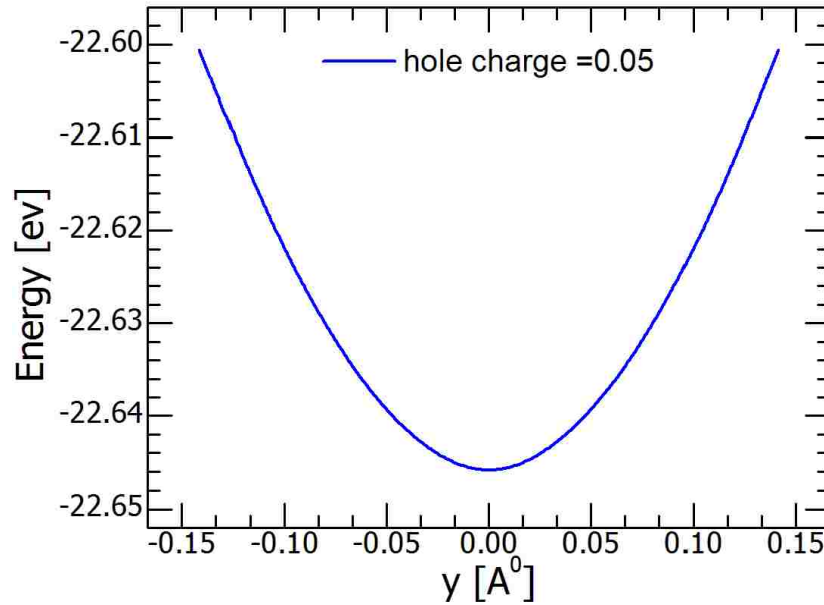
Figure 4.8. Elastic energy with hole doping of 0.05 for x=0
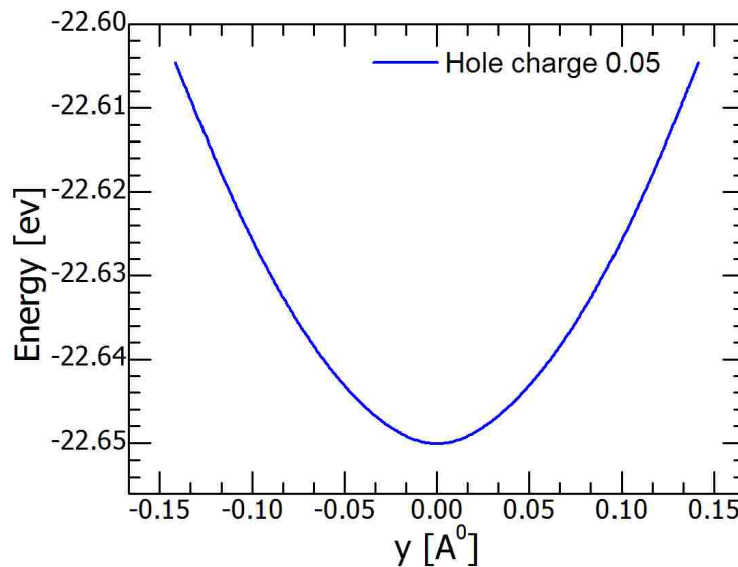
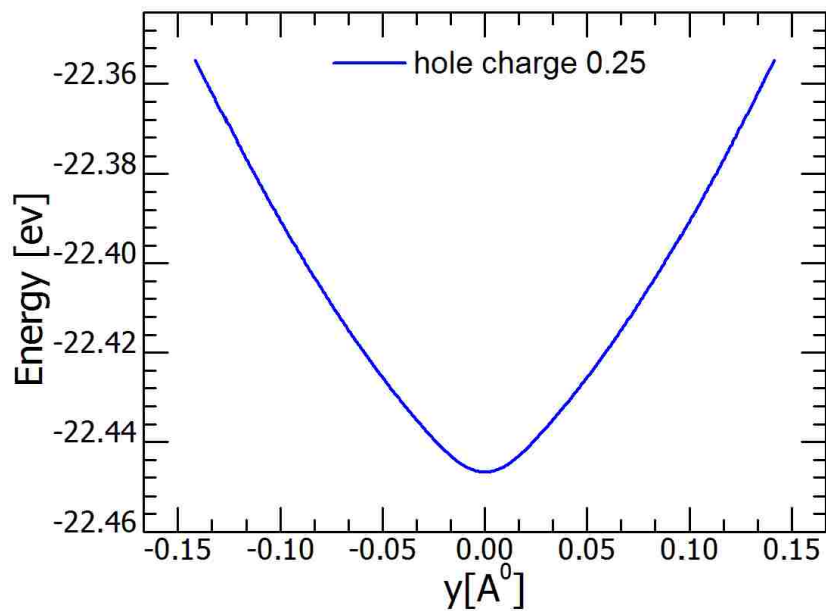**Figure 4.9. Elastic energy with hole doping of 0.05 for a constant x at minima**

Figure 4.10. Elastic energy with hole doping of 0.25 for x=0
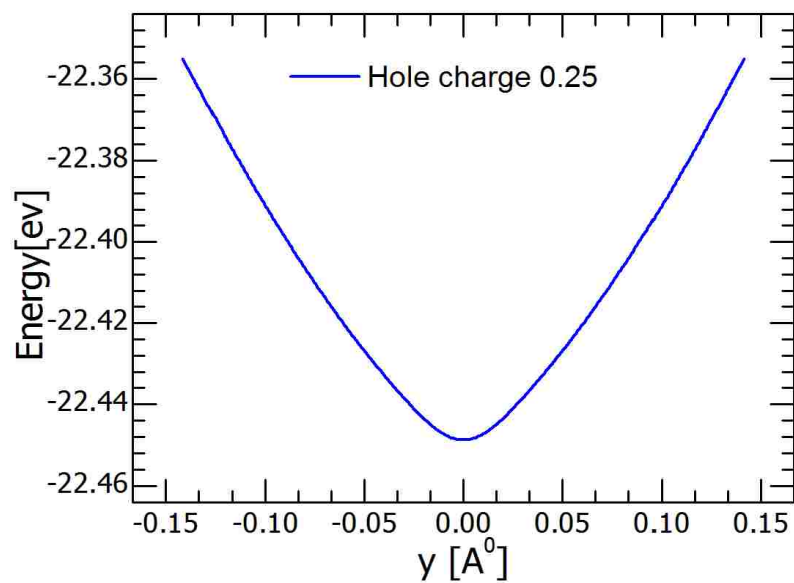
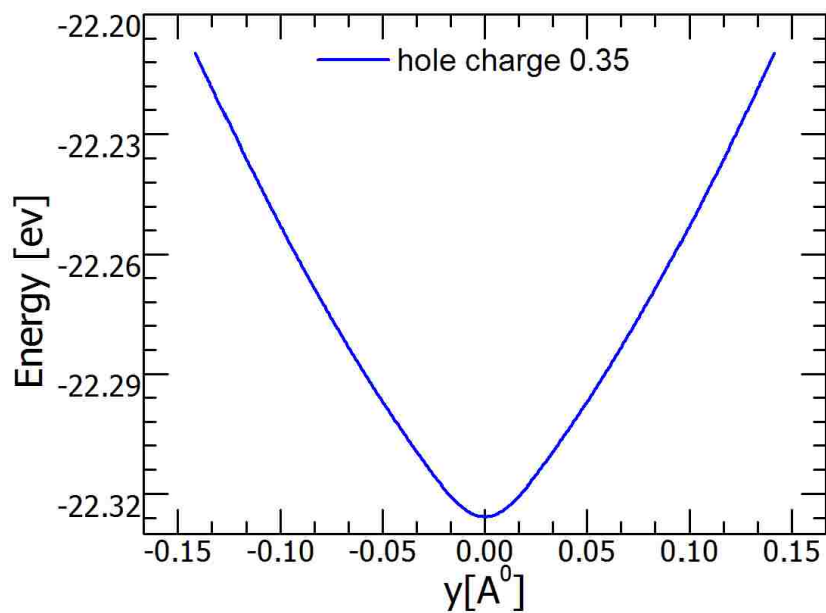**Figure 4.11. Elastic energy with hole doping of 0.25 for a constant x at minima**

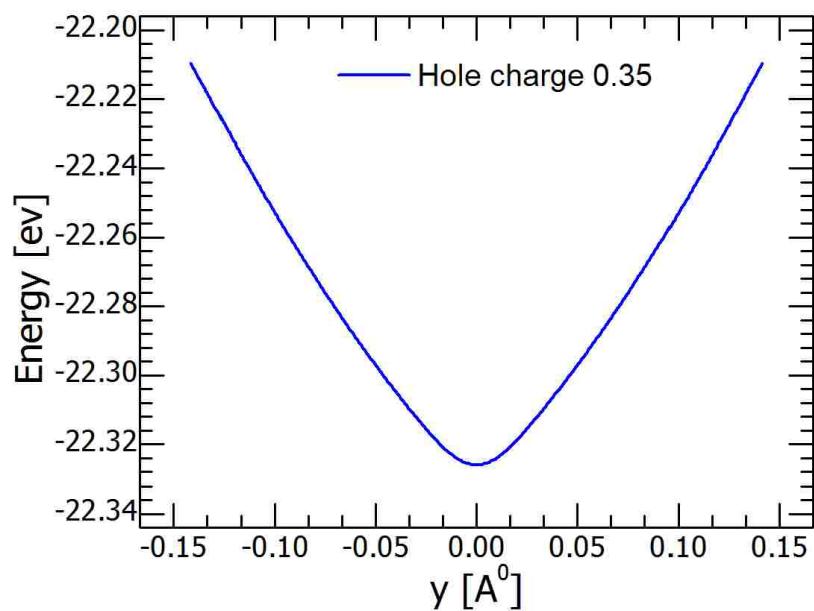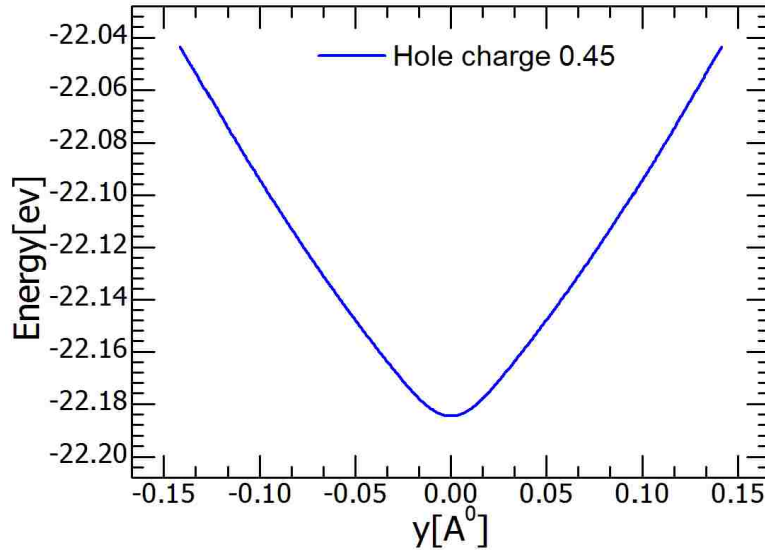**Figure 4.12. Elastic energy with hole doping of 0.35 for x =0**

Figure 4.13. Elastic energy with hole doping of 0.35 for a constant x at minima

Figure 4.14. Elastic energy with hole doping of 0.45 for x=0

The figure for elastic energy with hole doping of 0.45 for x =0 and at the minima are same since ground state structure and litharge structure are same. By applying strain and varying the lattice constants in y- direction and putting x=0 and putting x at a constant on minima, the effect on elastic energy has been observed. It has been found that for higher hole doping equation (4.8) becomes like this

$$U(x, y, q) = |a(q)|x^4 \text{-} |b(q)|x^2 + |e(q)|y + d(q) \tag{4.9}$$

Now putting x=0 and varrying lattice constants in y direction the coefficients c_1 and e_1 have been found for equation (4.8) and equation (4.9). Again, by fixing x at a constant value on minima and varrying lattice constants in y direction the coefficients c_2 and e_2 have been found for equation (4.8) and (4.9). By taking average of c_1 and c_2, the coefficeint c has been obtained for equation (4.8). Same way by taking average of e_1 and e_2 the coeffecent e has been obtained for equation (4.9). The following Table 3 shows hole charge per unit cell q with the coefficeints.

Table 3: q with associated $c_1, c_2, e_1 e_2$ c and e

$q(e)$	$c_1(^{ev}/_{A^2})$	$c_2(^{ev}/_{A^2})$	$c \ (^{ev}/_{A^2})$	$e_1(^{ev}/_{A})$	$e_2(^{ev}/_{A})$	$e(^{ev}/_{A})$
0.05	2.480800	2.474800	2.477800	0	0	0
0.25	0	0	0	0.716000	0.728000	0.722000
0.35	0	0	0	0.906400	0.908900	0.907700
0.45	0	0	0	1.102200	1.102200	1.102200

4.3 Elastic Energy of SnO with Electron Doping

The structural stability for n-type material has been assessed. The elastic energy has been calculated by applying strain and varying the lattice constants in x-direction with added electron dopants. Elastic energy has been calculated with electron doping from 0.01, 0.02, 0.03, and 0.04.

In the Table 4 electron charge per unit cell q, lattice parameters of litharge structure a_0 , litharge structure energy U_0, optimal rectangular structure (a_1, a_2), ground state energy U_g and energy difference between litharge structure and ground state energy ΔU for SnO monolayer have been provided.

Table 4: q, a_0 with associated energy U_0, (a_1, a_2) with associated energy U_g and ΔU (energy difference between U_g and U_0)

$q(e)$	$a_0 \ (A^0)$	U_0(ev)	$a_1(A^0)$	$a_2(A^0)$	U_g(ev)	ΔU(ev)
0.01	3.841663	-22.66753	3.995330	3.687997	-22.66876	0.001233
0.02	3.844072	-22.64692	3.988225	3.699920	-22.64787	0.000956
0.03	3.846523	-22.62621	3.971535	3.721511	-22.62693	0.000713
0.04	3.848771	-22.60545	3.954612	3.742930	-22.60597	0.000515

Again by applying strain and varying the lattice constants in x- direction and putting y=0, the coefficients a, b and d of equation (4.8) can be obtained for n type SnO monolayer. In the same way, by applying strain and varying the lattice constants in y- direction and putting x=0 the coefficient c_1 has been obtained. Fixing x at a constant value on the minima and varying lattice constants in y- direction, the coefficient c_2 has been obtained. By taking average of c_1 and c_2, the coefficient c of equation (4.8) has been obtained. The following Table 5 shows the electron charge per unit cell q with associated coefficients.

Table 5: q with associated a ,b , c_1, c_2 c and d

$q(e)$	a $(^{ev}/_{A^4})$	b $(^{ev}/_{A^2})$	$c_1(^{ev}/_{A^2})$	$c_2(^{ev}/_{A^2})$	$c(^{ev}/_{A^2})$	d (ev)
0.01	0.317200	-0.038000	1.893500	1.859300	1.876400	-22.668000
0.02	0.278800	-0.032700	1.800900	1.772200	1.786600	-22.648000
0.03	0.239000	-0.026400	1.708200	1.687300	1.697600	-22.626000
0.04	0.200100	-0.019900	1.615600	1.592300	1.604000	-22.605000
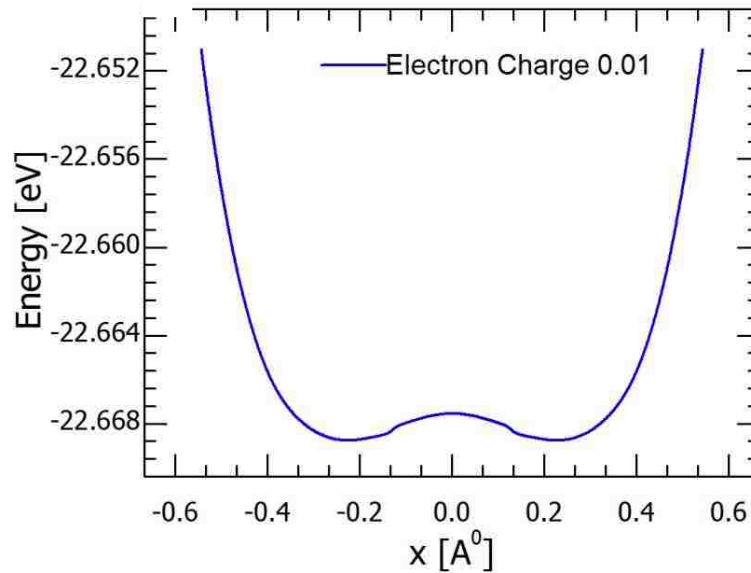
Figure 4.15. Elastic energy with electron doping of 0.01 for y =0
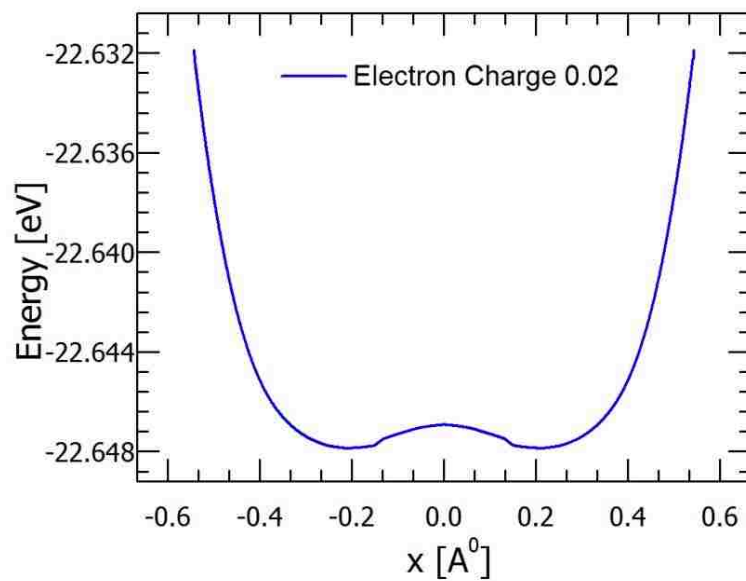
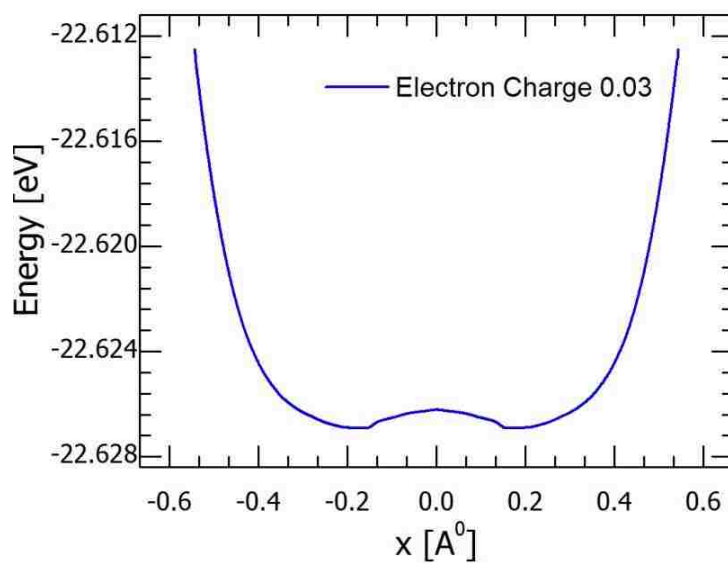**Figure 4.16. Elastic energy with electron doping of 0.02 for y =0**

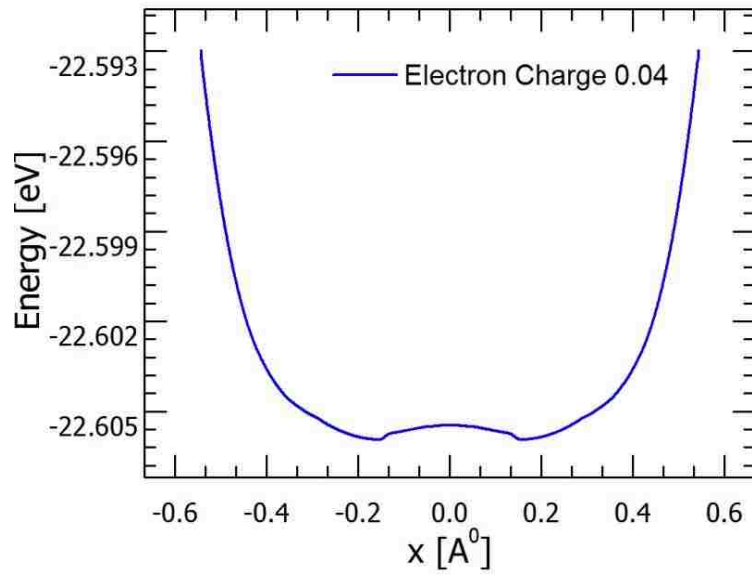**Figure 4.17. Elastic energy with electron doping of 0.03 for y =0**

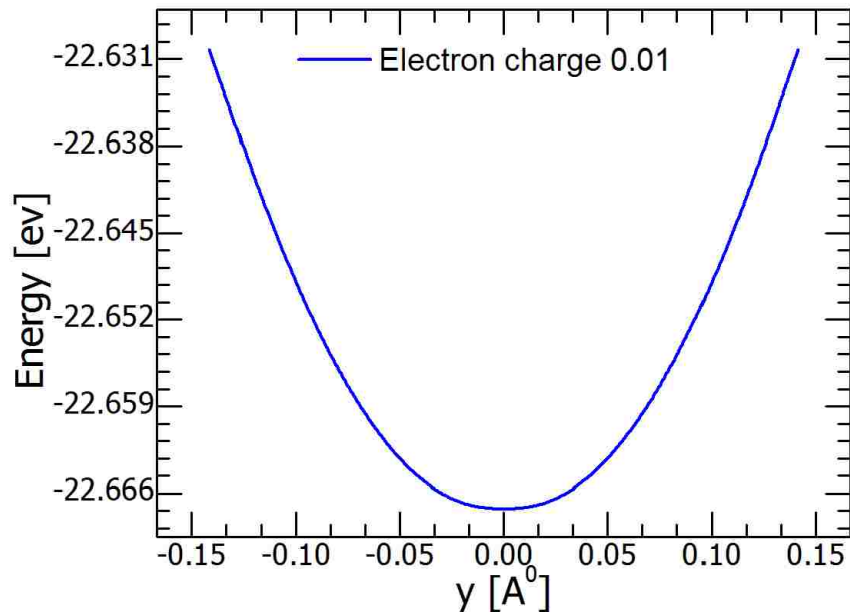**Figure 4.18. Elastic energy with electron doping of 0.04 for y =0**

Figure 4.19. Elastic energy with electron doping of 0.01 for x=0
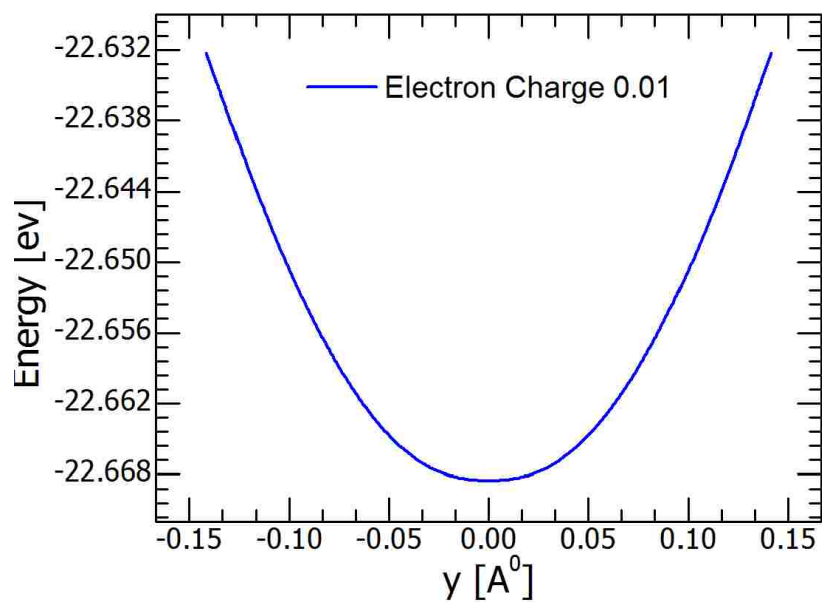
Figure 4.20. Elastic energy with electron doping of 0.01 for a constant x at minima
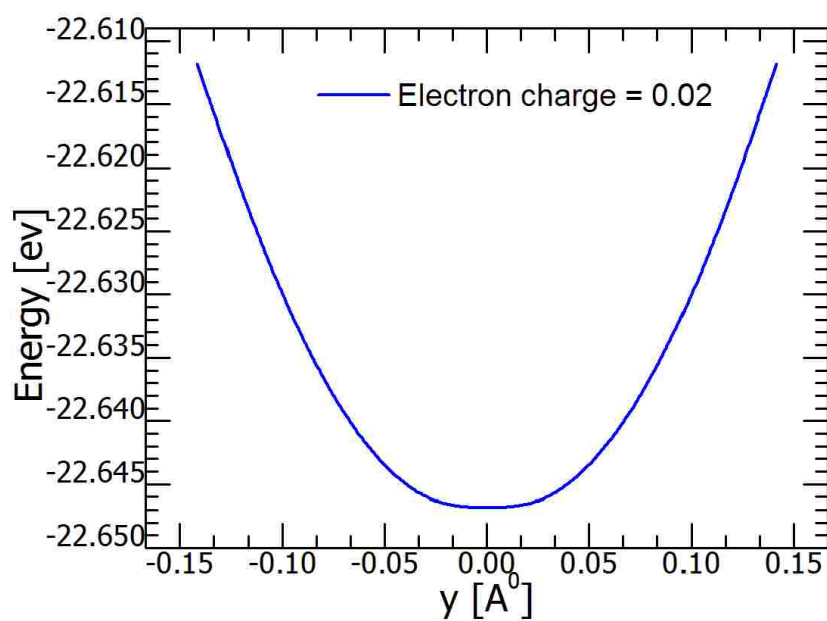

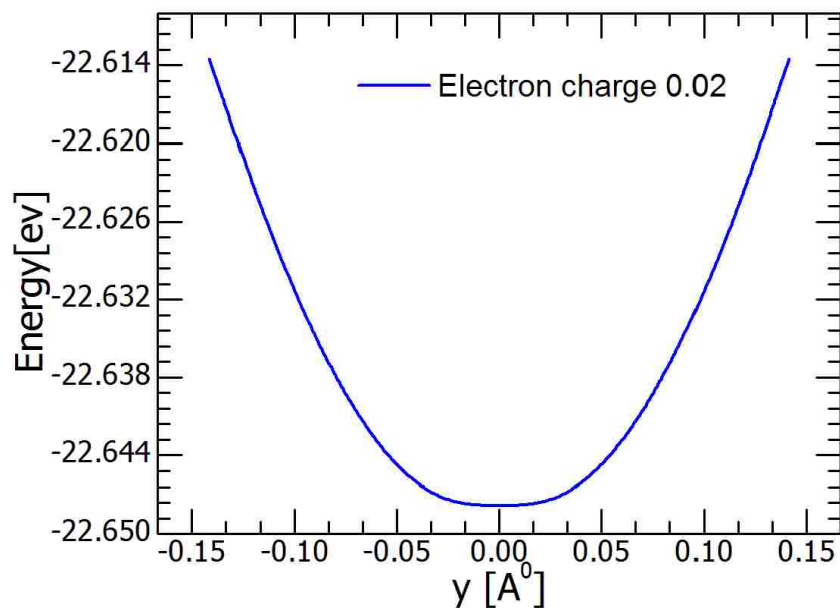**Figure 4.21. Elastic energy with electron doping of 0.02 for x=0**

Figure 4.22. Elastic energy with electron doping of 0.02 for a constant x at minima
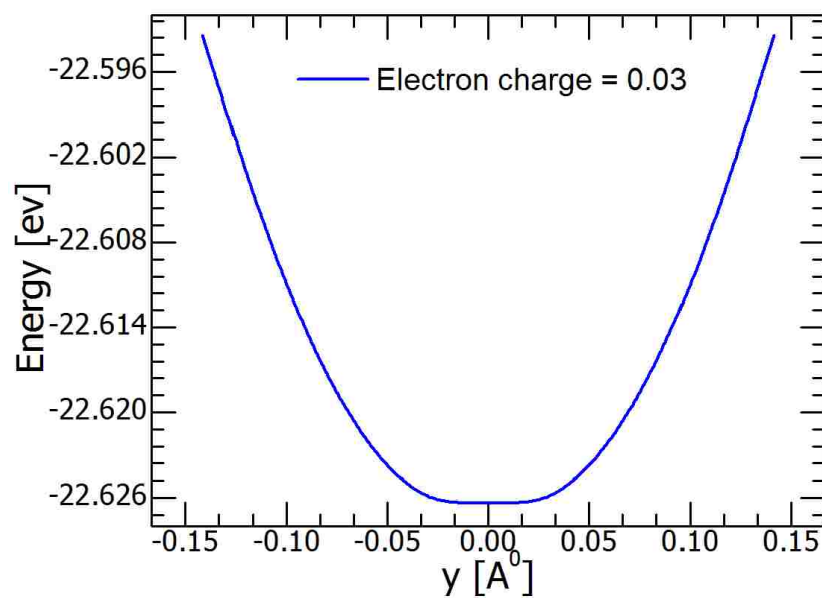

Figure 4.23. Elastic energy with electron doping of 0.03 for x=0
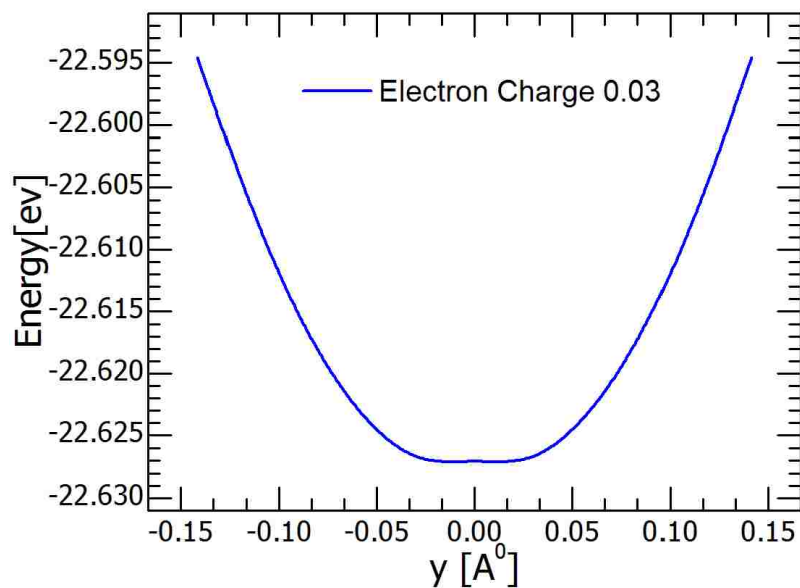
Figure 4.24. Elastic energy with electron doping of 0.03 for a constant x at minima
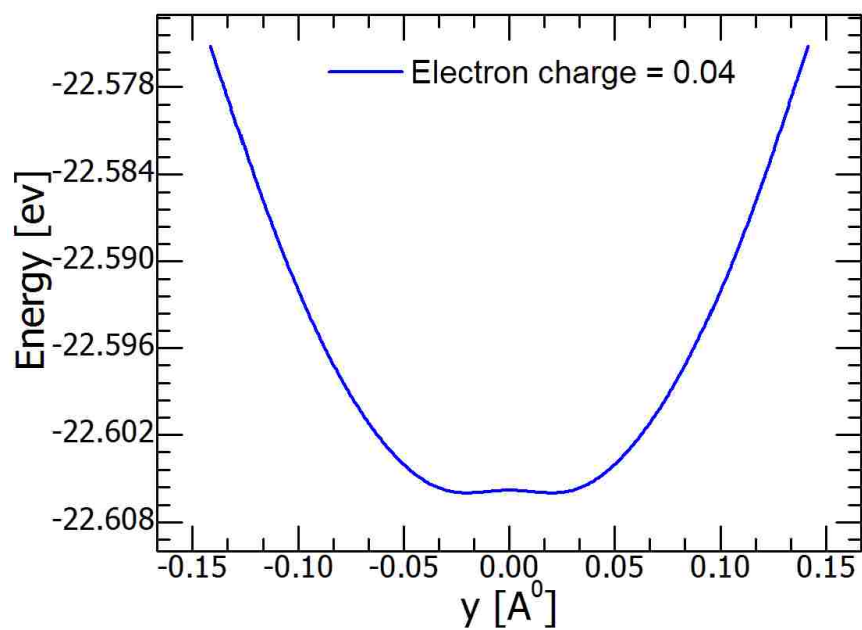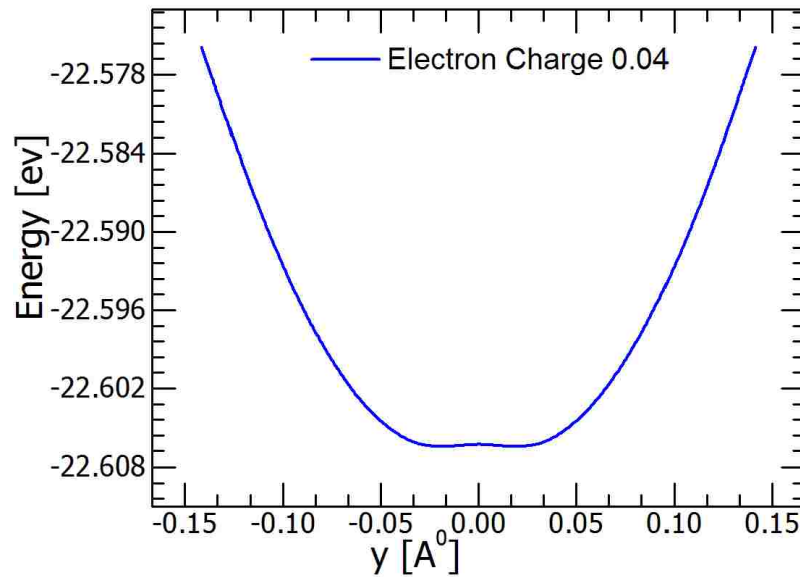

Figure 4.25. Elastic energy with electron doping of 0.04 for x=0

Figure 4.26. Elastic energy with electron doping of 0.04 for a constant x at minima

From the Table 4, it can be inferred that with increasing electron doping, the ground state energy increases. With the changing electron doping like hole doping, the energy difference between ground state and litharge structure state ΔU can be controlled and with increasing electron doping, ΔU starts to decrease, however for electron doping ΔU never reaches to zero. Unlike hole doping, electron doping ΔU does not reach to zero, so the ground state is always rectangular. Comparing Table 1 and Table 4, it can be seen that increase in ground state energy because of electron doping is faster than that in hole doping. Again from Table 5 it can be seen that varying lattice constants in x- direction and putting y =0, the anharmonic analytical expression (4.8) is always anharmonic while for hole doping of 0.45, that expression becomes harmonic.

CHAPTER 5

CONCLUSION AND FUTURE WORK

5.1 Conclusion of This Work

In summary, an analytical model has been developed for our understanding towards a complete picture of how properties of two-dimensional materials are affected by two dimensional structural transitions at finite temperature. The pre and post structural transition properties of neutral SnO monolayer such as the transition temperature Tc, which can signal a sudden change or shift in the structural order parameters, the elastic energy, and elastic parameters has been extracted in this thesis. Comparing of these parameters, the transition temperature has been obtained 19.3K for charge neutral SnO monolayer. The energy landscape of doped SnO monolayer and analytical model and coefficients for them have been also achieved in this thesis.

5.2 Future Work

In order to further enhance our understanding, Molecular Dynamics calculation can be done to get the transition temperature for charge neutral SnO so that the structural order parameters can be extracted. It will eventually increase our understanding on the pre and post structural parameters for vast numbers of molecules of SnO.

REFERENCES

[1] P. J. Chen, H.T. Jeng, "Phase Diagram of the layered Oxide SnO: GW and electron-phonon studies," *Scientific Reports* 5, 16359, 2015.

[2] X. Mao, A. Souslov, C. I. Mendoza, and T. C. Lubensky, "Mechanical instability at finite temperature," *Nature Communications* 6 ,5968, 2015.

[3] A. von Hippel, " Ferroelectricity, Domain Structure, and Phase Transitions of Barium Titanate," *Rev. Mod. Phys.* 22, 221, 1950.

[4] D. Khomskii,"Trend:Classifying multiferroics: Mechanisms and effects,"*Physics* 2, 20 2009, https://physics.aps.org/articles/v2/20.

[5] L. Seixas, A. S. Rodin, A. Carvalho, and A. H. Castro Neto, "Multiferroic two-dimensional materials", *Phys. Rev. Lett.* 116, 206803 ,2016.

[6] M. Mehboudi, A. M. Dorio, W. Zhu, A. van der Zande, H. O. H. Churchill, A. A. Pacheco-Sanjuan,E. O. Harriss, P. Kumar, and S. Barraza-Lopez, " Two-Dimensional Disorder in Black Phosphorus and Monochalcogenide Monolayers ," *Nano Letters* 16, 1704, 2016.

[7] M. Mehboudi, B. M. Fregoso, Y. Yang, W. Zhu,A. van der Zande, J. Ferrer, L. Bellaiche, P. Kumar, and S. Barraza-Lopez, "Structural phase transition and material properties of few-layer monochalcogenides," *Phys. Rev. Lett.* 117, 246802, 2016.

[8] R. Fei, W. Kang, and L. Yang, "Ferroelectricity and Phase Transitions in Monolayer Group-IV Monochalcogenides," *Phys. Rev. Lett.* 117, 097601, 2016.

[9] K. Novoselov, A. K. Geim, S. Morozov, D. Jiang, M. K. I. Grigorieva, S. Dubonos and A. Firsov, "Two-dimensional gas of massless Dirac fermions in graphene," *Nature,* vol. 438, pp. 197-200, 2005.

[10] R.Lieth,"Preparation & Crystal Growth of Material with Layered Structure,"*Springer*,1977.

[11] H. Boehm, R. Setton and E. Stumpp, "Nomenclature and terminology of graphite intercalation compounds," *Carbon*, vol. 24, pp. 241-245, 1986.

[12] E. Rokuta, Y. Hasegawa, K. Suzuki, Y. Gamou, C. Oshima and A. Nagashima, "Phonon dispersion of an epitaxial monolayer film of hexagonal boron nitride on Ni (111)," *Phys. Rev. Lett.*, vol. 79, pp. 4609, 1997.

[13] H. Liu, A. T. Neal, Z. Zhu, D. Tomanek and P. D. Ye, "Phosphorene: A New 2D Material with High Carrier Mobility," arXiv Preprint arXiv:1401.4133, 2014.

[14] B. Radisavljevic, A. Radenovic, J. Brivio, V. Giacometti and A. Kis, "Single-layer MoS_2 transistors," Nature Nanotechnology, vol. 6, pp. 147-150, 2011.

[15] X. Huang, Z. Yin, S. Wu, X. Qi, Q. He, Q. Zhang, Q. Yan, F. Boey and H. Zhang, "Graphene-Based Materials: Synthesis, Characterization, Properties, and Applications," Small, vol. 7, pp. 1876-1902, 2011.

[16] R. Mas-Balleste, C. Gomez-Navarro, J. Gomez-Herrero and F. Zamora, "2D materials: to graphene and beyond," *Nanoscale*, vol. 3, pp. 20-30, 2011.

[17] L. Xian, S. Barraza-Lopez and M. Chou, "Effects of electrostatic fields and charge doping on the linear bands in twisted graphene bilayers," Physical Review B, vol. 84, pp. 075425, 2011.

[18] M. I. Katsnelson, "Graphene: carbon in two dimensions," Materials Today, vol. 10, pp. 20-27, 2007.

[19] Bhimanapati, G. R.; Glavin, N. R.; Robinson, J. A., Francesca Iacopi, John J. Boeckl and Chennupati Jagadish, ed. Semiconductors and Semimetals. 2D Materials. 95. Elsevier. pp. 101–147, 2016.

[20] Li, Lu Hua; Chen, Ying , "Atomically Thin Boron Nitride: Unique Properties and Applications," *Advanced Functional Materials.* 26 (16): 2594–2608, 2016.

[21] http://cms.mpi.univie.ac.at/vasp/guide/vasp.html

[22] X. Mao, A. Souslov, C. I. Mendoza, andT. C. Lubensky, Nat. Comms. 6, 5968 (2015). http://www.nature.com/articles/ncomms6968.

APPENDIX A : VITA

Graduate School
University of Arkansas

AFSANA SHARMIN

asharmin@uark.edu

Southern Illinois University Carbondale
M.S., Electrical and Computer Engineering, 2013.

Thesis Title:
STRUCTURAL AND ELASTIC PROPERTIES OF DEGENERATE SNO MONOLAYERS AT FINITE TEMPERATURE

Major Professor: Dr. Salvador Barraza Lopez